Atmos. Chem. Phys. Discuss., 14, 26619–26653, 2014
www.atmos-chem-phys-discuss.net/14/26619/2014/
doi:10.5194/acpd-14-26619-2014

Atmospheric Chemistry and Physics Discussions

AOD trends during 2001–2010 from observations and model simulations

A. Pozzer[1], A. de Meij[2], J. Yoon[1], H. Tost[3], A. K. Georgoulias[4,5], and M. Astitha[6]

[1]Atmospheric Chemistry Department, Max-Planck Institute for Chemistry, Mainz, Germany
[2]Noveltis, Sustainable Development, Rue du Lac, 31670 Labege, France
[3]Institute for Physics of the Atmosphere, Johannes Gutenberg University Mainz, Germany
[4]Department of Meteorology and Climatology, School of Geology, Aristotle University of Thessaloniki, Greece
[5]Multiphase Chemistry Department, Max-Planck Institute for Chemistry, Mainz, Germany
[6]University of Connecticut, Civil and Environmental Engineering, Storrs, Connecticut, USA

Received: 1 September 2014 – Accepted: 6 October 2014 – Published: 23 October 2014

Correspondence to: A. Pozzer (andrea.pozzer@mpic.de)

Published by Copernicus Publications on behalf of the European Geosciences Union.

Abstract

The aerosol Optical Depth (AOD) trend between 2001–2010 is estimated globally and regionally from observations and from model simulations. The model is able to reproduce quantitatively the AOD trends as observed by MODIS satellite sensor, while some discrepancies are found when compared to MISR and SeaWIFS observations. Thanks to an additional simulation without any change in the emissions, it is shown that decreasing AOD trends over the US and Europe are due to decrease in the emissions, while over the Sahara Desert and the Middle East region the meteorological changes do play a major role. Over South East Asia, both meteorology and emissions changes are equally important in defining AOD trends. Additionally, decomposing the regional AOD trends into individual aerosol components reveals that the soluble components are the most dominant contributers to the total AOD, as their influence on the total AOD is enhanced by the aerosol water content.

1 Introduction

The atmosphere is a mixture of various gases and aerosols. The increase of greenhouse gases causing climate change is partially countered or enhanced by aerosol radiation modifications (the aerosol direct effect; Andreae et al., 2005). Additionally, aerosols can modify cloud properties (indirect effects; Ramanathan et al., 2001a, b; Kaufman et al., 2002). Furthermore, depending on their composition aerosols affect the ecosystems, quality of life (cardiovascular and respiratory diseases; Lelieveld et al., 2013) and visibility. Since the late 1980s the decline in solar radiation at the Earth's surface due to aerosol pollution (dimming) has reversed over the Northern Hemisphere (Wild et al., 2005; Wild, 2010). This change from dimming to brightening has important consequences for climate change, affecting the hydrological cycle, cloud formation processes and surface temperatures, possibly intensifying the warming trend caused by carbon dioxide (CO_2) and other greenhouse gases. Remote sensing instruments and

ACPD
14, 26619–26653, 2014

Atmospheric Chemistry Transport Models (ACTMs) provide possibilities for improved qualitative and quantitative analysis of the global burden of atmospheric trace gases and aerosol particles. ACTMs and chemistry climate models (CCMs) are additionally used to assess the effects of future changes in aerosol (+ precursor) emissions on climate by making use of physical and chemical process descriptions in dependency of emission inventories. These emission inventories are constructed from estimates for population and economic growth to determine present gas phase and aerosol emissions as well as future emission scenarios. The emission inventories include natural and anthropogenic emissions relevant for aerosol formation, such as sulphur dioxide (SO_2), nitrogen oxides (NO_x), black (BC) and organic (OC) carbon, ammonia (NH_3) and many more compounds.

SO_2 and BC are mainly emitted from fossil fuel (coal and petroleum) combustion. Primary sources for NO_x are road transport and fossil fuel combustion for energy production, and NH_3 is mainly emitted from agricultural activities (waste burning and fertilizers) and to a small extent by the combustion of biofuels for energy use. The amount of NH_3 emitted by agricultural activities is related to the type of fertilizer, meteorological conditions (wet/dry) and soil properties.

Since 1990 in Europe and in North America the emissions of aerosol precursors have dropped in response to the implementation of air quality legislation (Clean Air Act Amendments), which aims to reduce the emissions of sulfur dioxide (SO_2) and nitrogen oxides (NO_x). Despite the implementation of the 11th Five Year Plan (2006–2010) of State Environment Protection Administration (SEPA) in China, which requires power plants to implement new air pollution reduction technologies after 2006, air pollution remains a major concern in this region (Cao et al., 2009). Half of China's SO_2 emissions are attributed to the burning of coal, mostly by power plants, which are to a large degree located in the eastern part of the country where the large cities are situated. Between 2001 and 2005, SO_2 emissions still increased by 27 % (11th Five Year Plan, SEPA, March 2006). Lu et al. (2010) found an increase in SO_2 of 53 % between 2000 and 2006 (with annual growth rate of 7.3 %), with 85 % in the North and 28 % in the South of the

ACPD
14, 26619–26653, 2014

country. The increase has been reduced after 2006, due to the implementation of new emission reduction technologies (i.e. desulfurization) in power plants. SO_2 emissions in China do not show a strong seasonal cycle (Zhang et al., 2009), because of the continual energy production for industry and domestic usage.

Previous studies by Ohmura (2009); Long et al. (2009); Norris and Wild (2009) have investigated the global and regional solar radiation budget by using observations of the Global Energy Balance Archive (GEBA). Other studies have used various satellite products to investigate the impact of air pollution on the incoming solar radiation at the Earths surface (dimming and brightening phenomena), such as Wild et al. (2005), Wild (2010, special issue J. Geophys. Res., and references therein), Pinker et al. (2005); Hinkelman et al. (2009); Mishchenko and Geogdzhayev (2007); Remer et al. (2008); Chylek et al. (2007); Lu et al. (2010); Zhang and Reid (2010) and Kishcha et al. (2009). These studies have shown elevated AODs (decreasing incoming solar radiation at Earths surface) over India, East Asia, Bay of Bengal, Arabian Sea and reduced AODs (increasing incoming solar radiation) over North America and Europe.

A recent work of Hsu et al. (2012) with the SeaWIFS instrument has shown high precision in trend derivation while reporting decreasing trends over the eastern USA and Europe and increasing trends over China and India. Hsu et al. (2012) additionally have investigated the impacts of other uncertainty factors in trend estimates, e.g. retrieval algorithm deficiency and sampling bias, by comparing their results with AERONET and MODIS-Terra products. In particular the correlation analysis between large-scale meteorological events (such as El Niño Southern Osciallation and North Atlantic Oscillation) and SeaWiFS-retrieved AOD indicated strong influences of the climatic indices on Saharan dust outflow and biomass-burning activity in the tropics.

In de Meij et al. (2012a) the trends in AODs by remote sensing instruments have been investigated and linked to the changes of the aerosol (precursors) emissions in different emission inventories. They have found significant decreasing trends in observed AODs by MODIS, MISR and AERONET over Western Europe and North-East America between 2000–2009, associated with the reported negative trends in SO_2,

ACPD
14, 26619–26653, 2014

NH_3 and NO_x emissions. Positive AOD trends have been found over parts of Asia. However, no model simulations have been performed to quantify the changes in the aerosol (precursors) emissions on aerosol and AOD trends. In the present study we relate the chemical reactions of the gas and aerosol species on the trends in the simulated AODs and compare them with observations. A recent study by Chin et al. (2014) assessed the aerosol variations and trends over a period of 30 years. They used the GOCART model on 2.5°×2° horizontal resolution, with ACCMIP and RCP8.5 emissions. Two simulations were performed, one with all natural and anthropogenic emissions and the second one with no anthropogenic emissions. They have found that changes in calculated AODs are consistent with the changes in the emissions. They also have reported that for global averaged AOD values no significant trend could be identified and that analysis on regional scale is required. However, one must be careful in the conclusions as the annihilation method (i.e. removing all the anthropogenic emissions, in this case) could lead to strong effects due to the non-linearities (e.g. chemistry, aerosol microphysics) inherent in the climate system.

The objective of this work is to investigate the causes of AOD trends over different regions of the world, especially linking the trends to changes of natural/anthropogenic emissions or changes in atmospheric dynamics. To achieve this objective, two different simulations were performed: (a) anthropogenic and biomass burning emissions change realistically during the decade 2001–2010 and (b) anthropogenic and biomass burning emissions are kept constant and are equivalent to the year 2000 (i.e. with no inter-annual emission variability).

To our knowledge no work has been reported comparing the AOD trends from satellite measurements with model simulation with and without changing emissions for the decade 2001–2010 on global scale. This work clearly defines the causes of significant AOD trends for some regions.

In the next section the model used in this study is presented (Sect. 3), followed by the description of the analyzed observational dataset. In Sect. 4 the model results are compared with observations to evaluate its capability to reproduce AOD and AOD

ACPD
14, 26619–26653, 2014

trends. The AOD trends in global and regional scale are analyzed in Sect. 5, and the causes of AOD trends for specific regions are discussed in details in Sect. 6. The conclusions are summarized in Sect. 7.

2 Model description and setup

The ECHAM/MESSy Atmospheric Chemistry (EMAC) model is a numerical chemistry and climate simulation system that includes sub-models describing tropospheric and middle atmosphere processes and their interaction with oceans, land and human influences (Jöckel et al., 2010). It uses the second version of the Modular Earth Submodel System (MESSy2) to link multi-institutional computer codes. The core atmospheric model is the 5th generation European Centre Hamburg general circulation model (ECHAM5, Roeckner et al., 2006). For the present study we use ECHAM5 version 5.3.02 and MESSy version 2.42.

The EMAC model has been extensively evaluated for gas tracers (e.g. Pozzer et al., 2007) and for aerosols (e.g. Pringle et al., 2010a; Pozzer et al., 2012; Astitha et al., 2012).

The modeled AOD is calculated at 550 nm using concentrations of dust and sea salt particles, biomass burning products (black carbon and organic carbon) and anthropogenic aerosols (sulphates, nitrates, etc). The aerosol optical properties are calculated with the EMAC submodel AEROPT, which is based on the scheme by (Lauer et al., 2007) and makes use of predefined lognormal modes (i.e. the mode width σ and the mode mean radius have to be taken into account). Lookup tables with the extinction coefficient, the single scattering albedo and the asymmetry factor for the shortwave and extinction coefficient for the longwave part of the spectrum are pre-calculated with explicit radiative transfer calculations (see Pozzer et al., 2012). The considered compounds are organic carbon, black carbon, dust, sea salt, water-soluble compounds (WASO, i.e. all other water soluble inorganic ions, e.g.: NH_4^+, SO_4^{2-}, HSO_4^-, NO_3^-) and aerosol water (H_2O).

ACPD
14, 26619–26653, 2014

Previous studies using the EMAC model have proven that the simulated AOD is able to capture the overall global pattern although a general underestimation is present (de Meij et al., 2012b; Pozzer et al., 2012). The seasonal cycle of AOD is in general well represented in the EMAC model simulations in most parts of the globe, especially over dust influenced regions. In heavily anthropogenic polluted regions, the modeled AOD is slightly overestimating the observations.

In this study, the Chemistry Climate Model (CCM) EMAC has been used with a T63L31 resolution, corresponding to a horizontal resolution of $\approx 1.75^{\circ} \times 1.75^{\circ}$ of the quadratic Gaussian grid, and with 31 level vertical levels up to 10 hPa in the lower stratosphere. The model set-up used in this work was presented by Pozzer et al. (2012), and here only the differences and the central features are described.

The atmospheric chemistry is simulated with the MECCA (Module Efficiently Calculating the Chemistry of the Atmosphere) submodel by Sander et al. (2005, 2011), while the aerosol microphysics and gas-aerosol partitioning are calculated by the Global Modal-aerosol eXtension (GMXe) aerosol module (Pringle et al., 2010a, b). For descriptions of the emission and deposition routines we refer to Kerkweg et al. (2006a, b); Pozzer et al. (2006) and Tost et al. (2007).

As in Pozzer et al. (2012) and Pringle et al. (2010a), both dust and sea-salt emissions are offline prescribed using offline monthly emission files based on AEROCOM and do not depend on the model meteorology, hence having no multi-annual variability. However, the desert dust and sea salt aerosol concentrations that influence the AOD calculation exhibit multi-annual variability as the model description of the aerosol microphysical process (coagulation, condensation, ageing) as well as transport (advection, convection) and deposition processes are subject to meteorological variability.

The biomass burning contribution was added using the Global Fire Emissions Database (GFED version 3, van der Werf et al., 2010) with a monthly temporal resolution.

In this work we used the emissions scenarios recently developed for the ACCMIP (Atmospheric Chemistry and Climate Model Intercomparison Project, www.giss.nasa.

ACPD
14, 26619–26653, 2014

gov/projects/accmip/) initiative, which focuses on emissions scenarios based on the Representative Concentration Pathways (RCP) (Lamarque et al., 2011; Meinshausen et al., 2011; van Vuuren et al., 2011b, a, and references therein). The RCPs consist of four emission scenarios, also called RCP 2.6, 4.5, 6.0, and 8.5 representing the radiative forcing of anthropogenic activity from 2.6 to 8.5 $W\,m^{-2}$ in 2100, which depend on the mitigation or emission scenarios. Among them, the emission scenario RCP 8.5 is used in this study as Granier et al. (2011) showed that it is a "reasonable" choice for anthropogenic emissions after the year 2000 and for the recent past.

In this work two simulation were performed covering the year 2000–2010:

- a simulation named RCP85, where the anthropogenic emissions were based on the RCP 8.5 scenario and the biomass burning were based on the GFED emissions (e.g., with annual variability of the emissions);
- a simulation named RCP00, where the anthropogenic and biomass burning emissions were kept constant during all the simulation and equivalent to the year 2000 (i.e. with no interannual variability of the emissions).

Additionally, to compare the different simulations, the chemistry and the dynamics have been decoupled, such that there is no direct interaction and feedback between the atmospheric composition of the gas phase and aerosol particles with the dynamics of the atmosphere.

Accordingly, both simulations follow the same (i.e. binary identical) dynamics and meteorology, i.e. the CCM is used as a chemistry-transport model. The model dynamic has been weakly nudged (Jeuken et al., 1996; Jöckel et al., 2006) towards the analysis data of the European Centre for Medium-Range Weather Forecasts (ECMWF) operational model to represent the actual day-to-day meteorology in the troposphere, which allows a direct comparison of the simulations results with observations.

Although the simulations cover the period 2000–2010, the first year is used as spinup time, and the results of this work are based on 10 years of data (2001–2010). Additionally, the submodel SORBIT (Jöckel et al., 2010) was used to sample the AOD at the

ACPD
14, 26619–26653, 2014

correct local time of the satellite overpass. Hence, we can neglect any influence of the diurnal cycle in the comparisons performed in the next sections.

3 Remote sensing data

In this work, observations from three different satellite sensors have been analyzed independently. Specifically, the following satellite datasets have been used:

- The Multi-angle Imaging SpectroRadiometer (MISR) instrument (Diner et al., 1998) is located onboard the Terra satellite and has been operational since February 2000. The instrument is designed to measure the solar radiation reflected by the Earth–Atmosphere system by a multiple camera configuration (four forward, one nadir and four backward). Each camera measures in four different wavelengths centered at 446 nm (blue), 558 nm (green), 671 nm (red) and 866 nm (near-infrared). In this study, Level 3 Component Global Aerosol Product version F15 (CGAS-F15) data are used. Specifically the AOD (Aerosol Optical Depth) retrievals at 558 nm from the Level 2 product are averaged on a monthly basis and stored on a geographic grid of 0.5° × 0.5°. The validation of MISR AODs over land and ocean with AERONET (AErosol RObotic NETwork) data has shown that MISR retrievals are within 0.05–20 % of that of AERONET (Kahn et al., 2005, 2010).

- The MODerate resolution Imaging Spectroradiometer (MODIS) sensor is also located on the Terra satellite. In contrast to MISR, the MODIS instrument has only one camera which measures radiances in 36 spectral bands. MODIS aerosol products are provided over land (Kaufman et al., 1997) and water surfaces (Tanré et al., 1997) with uncertainties being $\pm 0.05 \pm 0.15 \times$ AOD (Chu et al., 2002; Remer et al., 2008; Levy et al., 2010) and $\pm 0.03 \pm 0.05 \times$ AOD (Remer et al., 2002, 2005), respectively. In this paper, AOD550 data from the MODIS Level 3 (Col 051) gridded product are used at a spatial resolution of 1° × 1°.

ACPD
14, 26619–26653, 2014

– The Sea-WIFS (Sea-Viewing Wide Field-of-View Sensor) instrument operated on board GeoEye's OrbView-2 (AKA SeaStar) satellite providing data from September 1997 to December 2010. AODs at different wavelengths have been retrieved over land with the use of the Deep Blue algorithm over land (Hsu et al., 2004, 2006) and ocean using the SeaWiFS Ocean Aerosol Retrieval (SOAR) algorithm (Sayer et al., 2012a) at a horizontal resolution of ∼ 13.5 km. Here, SeaWiFS v003 Level 3 AOD550 gridded data are used at a spatial resolution of $1^{\circ} \times 1^{\circ}$ following (Hsu et al., 2012). Validation studies of Sea-WIFS's AOD550 with ground-based observations from AERONET and data from other satellite sensors indicate an absolute expected error of 0.03 + 15 % over ocean and 0.05 + 20 % over land at 550 nm (Sayer et al., 2012a, b).

In addition to the satellite observations, AOD from station observations are also used in this work. The in situ AOD observations have been obtained from the global AErosol RObotic NETwork (AERONET Holben et al., 1998; Dubovik et al., 2000). The solar extinction measurements are used to calculate the aerosol optical depth with an accuracy of about 0.01–0.02 AOD units (Eck et al., 1999). The cloud-screened quality-assured Level 2 AOD data used in this work were obtained from the website http://aeronet.gsfc.nasa.gov/cgi-bin/combined_data_access_new, and contain AOD daily averages. Furthermore, the AOD at 550 nm was calculated from the AOD values reported at 870 and 440 nm by using the information of the Ångström exponent (see Eqs. 1 and 2, de Meij et al., 2012b).

4 Comparison of model results to AERONET observations

In this work the AERONET data is purely used for evaluation of the model performance, but no AOD trends will be estimated and compared with the model. In fact, the variable time coverage of the AERONET data make it difficult to have robust trend comparison for the simulation period, and therefore we refer to other studies on this issue (Yoon et al., 2012).

ACPD
14, 26619–26653, 2014

The model AOD product was extensively evaluated already in a number of publications (Pringle et al., 2010a; de Meij et al., 2012b; Pozzer et al., 2012; Astitha et al., 2012). In this section we compare briefly the model with in situ observations, to confirm the previous findings. As shown in Fig. 1, the model is generally able to correctly reproduce the AOD observed by AERONET, mostly within a factor of two. When the observed AODs are compared to the simulated AODs, it is interesting to notice that both simulations show similar linear fit: the correlation coefficients (0.57 and 0.52 for RCP85 and RCP00, respectively) and the bias (0.02 and 0.03 for RCP85 and RCP00, respectively) are very similar while the slope is almost equal to 1 for both simulations. This implies that the average global observed and calculated AODs do not vary significantly during 2001 and 2010, which corroborates the study by Chin et al. (2014). It also indicates that both simulations are in general able to reproduce the overall maxima/minima, although RCP85 shows slightly better agreement for correlation and slope of the linear fit. However, large differences are found in the AOD trends on a regional scale between RCP85 and RCP00 and this will be further discussed in the next sections.

5 AOD trends

5.1 AOD trends – geographic patterns

In Fig. 2 the global trends observed by MODIS, MISR and SeaWIFS instruments are shown. A simple linear model has been applied to estimate the trends following the work of (Weatherhead et al., 1998): $Y_t = \mu + \omega X_t + S_t + N_t$, where Y_t, μ, ω and X_t denote the monthly time series, the offset, the trend (i.e. AOD yr^{-1}), and the years of the time series ($X_t = t/12$ with t as month), respectively. S_t is a seasonal component representing the effect of the seasonal variations in the trends estimates, while N_t is the residual term of the interpolation. The seasonal component we have taken into account

ACPD
14, 26619–26653, 2014

is based on the Fourier series as proposed by Weatherhead et al. (1998, 2002) with: $S_t = \sum_{j=1}^{4}[\beta_{1,j}\sin(2\pi jt/12) + \beta_{2,j}\cos(2\pi jt/12)]$.

A statistically significant trend at 95 % confidence level is defined by the absolute value of the ratio of the trend to its SD which is larger than two (Tiao et al., 1990; Weatherhead et al., 1998), with the SD of the trend estimated again with the approach of Weatherhead et al. (1998, Eq. 2).

As already shown by de Meij et al. (2012a), "significantly negative trends are present over Europe and North America, whereas over South and East Asia they are mostly positive". More specifically, both MISR and SeaWIFS show a small significant decrease over North America and partially Europe, while strong increase is visible over Saudi Arabia. MODIS presents a much better spatial coverage (due to the almost daily global coverage), showing a strong reduction of the AOD in the decade 2001–2010 especially over East-USA, Europe and biomass burning regions, such as Central Africa and South East Asia. South Arabia shows a significant increasing trend, although this is not shown directly by MODIS, as no aerosol retrieval is possible over bright surfaces, such as deserts and ice.

In Fig. 3 the trends are estimated for both simulations (RCP00 and RCP85), using the same method as for the remote sensed observations. For both model simulations AOD data is sampled at the same co-located time of the observations, thanks to the submodel SORBIT (Sample along satellite ORBIT, Jöckel et al., 2010), following the trajectories of the platform TERRA (on which MODIS and MISR instruments are on board) and OrbView-2 (with the SeaWIFS instrument on board). It is clearly noticeable that the model results from simulation RCP85 generally are in agreement with the estimated trends from remote sensed observations, indicating that these trends are (in general) anthropogenically driven. These tendencies are consistent with the results in various studies based on trend analysis of satellite-retrieved AOD (e.g. Zhang and Reid, 2010; Hsu et al., 2012; Yoon et al., 2013). Since the satellite-retrieved AOD data, which have been used in most of the trend analyses, are only available under cloud-free

ACPD
14, 26619–26653, 2014

conditions, the trend estimates based on the cloud-free AOD products can be biased due to insufficient retrievals in cloudy seasons (Yoon et al., 2013).

The North American and European caculated trends are reproduced coherently with the observed ones and a significant increase of AOD in the simulation RCP85 can be observed also in the Saudi Arabian peninsula. In addition, a strong significant increase during the decade 2001–2010 is observed over East Asia, which is however not fully corroborated by the observations. The strong decreasing trend over the Tropical/Southern Africa is not well reproduced by the model.

The model results from simulation data RCP00 (see Fig. 3, left plots) do not show significant trends both in Europe and Northern USA, while they still do present significant trends both in Northern Africa (Sahara Desert) and South East Asia.

5.2 AOD regional trends

The global analysis of the AOD trends discussed in the previous section revealed regions of interest where the trends from either satellite instruments or model simulation RCP85 are significant and require further investigation. The 7 selected regions are Eastern United States (EUS), Western Europe (WE), Sahara desert (SD), Middle East (ME), South Asia (SA), East China (EC), and South East Asia (SEA) (illustrated in Fig. 4). The regional trend analysis is illustrated with scatter plots that show the comparison between the model and the satellite AOD trends (Fig. 5), each point representing the regional mean trend for the respective regions. The two model simulations (RCP00, RCP85) are equally important to investigate the effect of decadal emission changes during 2001–2010. By comparing the two model simulations, we obtain useful information about the contribution of the emissions to the positive or negative AOD trends. The first evident conclusion is that the trends calculated from the RCP85 simulation (varying emissions) compare well with the satellite trends in contrast with the RCP00 simulation (constant emissions). The correlation coefficients for the RCP85-satellite trends range between 0.73 and 0.87, whereas for the RCP00 the values are

ACPD
14, 26619–26653, 2014

significantly lower (0.32–0.41). This result alone gives a first insight on the importance of the emissions variation of the AOD within the time period under analysis.

Focusing on the target regions, over Western Europe (WE), the AOD trends are negative by the model simulations and the satellite retrievals, with RCP85 being closer to the satellite-based trend. This is related to the influence of the anthropogenic emissions regulation imposed in Western Europe that resulted in a decrease of the atmospheric aerosol load during the decade 2001–2010 (Vestreng et al., 2007, 2009). The same applies to Eastern US (EUS) with results by simulation RCP85 and observed AOD having a negative trend. Nevertheless, the model overestimates the negative trend by MISR and SeaWIFS and correlates better with the MODIS retrievals.

A common pattern appears in the AOD trends for the climatically sensitive region of Middle East (ME) by the model simulations and satellite data. The positive trends calculated from the observations (the three satellite products agree) are somewhat higher than predicted by the model, which shows a slightly positive trends in both simulations (RCP85 and RCP00). This means that the variation in the emissions did not affect the AOD trend in this region, which is mostly affected by desert dust emissions and the dynamic factors that control dust transport and deposition. In fact, the dust emissions were prescribed off-line in the model, i.e. independent on the wind fields and therefore independent on the meteorological conditions. Therefore, the positive trends in this region can be attributed to the decrease in the precipitation and the consequent reduction of wet scavenging of dust particles, phenomena already observed by several authors for the decade 2001–2010 (e.g. Shehadeh and Ananbeh, 2013; Philandras et al., 2011).

The same is confirmed by the Global Precipitation Climatology Project (GPCP), which shows a strong decrease in precipitation in this region during the period 2007–2010 (not shown). Finally, despite the increasing AOD trend in the region simulated by the model, this is still lower than what is estimated by the observations, due to (i) the constant emissions which do not include enough variability in the source areas (Astitha

ACPD
14, 26619–26653, 2014

et al., 2012), and (ii) lower precipitations decrease in the model simulations than the observed one for the period 2007–2010.

A similar behavior is found for the Sahara Desert (SD) region where the AOD trends remain unchanged between the two model simulations. The trends observed by the satellites exhibit a small variation (for MODIS is slightly negative; for MISR and SeaWIFS is slightly positive) which can be attributed to the different algorithm assumptions (Kahn et al., 2007, 2009), calibration methods, and differences in the aerosol models used to construct the lookup tables in the retrival algorithms (Abdou et al., 2005). Nevertheless, the difference in the trends is very small considering the high total AOD values in this region.

For South Asia (SA) and Eastern China (EC), the improved temporal correlation coefficients by the RCP85 simulations with the satellite trends shows the importance of the variability in the emissions compared to the constant emission assumption. The sign of the trend changes from negative (RCP00) to positive (RCP85) in the two simulations, which is due to the increase emissions of the fast developing countries like China and India. The high positive trends modeled by simulation RCP85 over EC deviate from the satellite trends and this can be explained by the influence of desert dust aerosols that is not accurately represented by the model simulations. In fact, the MODIS trends for the entire EC region are slightly negative whereas the sign is positive by both MISR and SeaWIFS (see Fig. 5). This could be attributed to uncertainties in the AOD retrieval, e.g. sensor calibration status, retrieval accuracy, and cloud contamination. In addition, insufficient sampling not reflecting actual data population due to different sampling times, limited orbital periods, and cloud occurrence, which can be serious over polluted and cloudy areas, could be another reason (see Yoon et al., 2013).

In South East Asia (SEA) the model (sampled on the TERRA platform overpass) calculated a statistically significant negative trend in RCP00 ($-1.77 \pm 0.6\,\%\,yr^{-1}$) caused by changes in the meteorological conditions. Interestingly, this trend is enhanced in RCP85 ($-3.03 \pm 1.65\,\%\,yr^{-1}$, not significant) due the changing biomass burning emis-

ACPD
14, 26619–26653, 2014

sions (Yoon and Pozzer, 2014) during this decade in the region. Therefore, AOD trend in this region seems to be caused both by meteorological and emissions changes during the decade.

6 Effects of aerosol components in modeled AOD trends

In this section the main causes of positive/negative trends in the regions of interest are analyzed. The trends for each of the regions defined in Sect. 5.2 are decomposed by estimating the AOD trends for the different aerosol components: black carbon (BC), organic carbon (OC), dust (DU), aerosol water (H_2O), sea salt (SS), water soluble compounds (WASO) (see Fig. 6 and Table 1). Additionally, in this section, the full model output was used, so that the results are based on the full 10 years model results.

In general, aerosol water content has the largest contribution to the total AOD and therefore must be considered as the most effective extinction component in the aerosol polluted atmosphere (Gao, 1996). In the Eastern part of the US and in the Western part of Europe, a decrease in the WASO components (i.e. ammonium, nitrate and sulphate) is found during the decade 2001–2010. The negative AOD trends are amplified, since not only the number of particles in the atmosphere has decreased, but also their water uptake efficiency and consequently the aerosol water content. This highlights the fact that the observed AOD trends depend on the reduction in the emissions (van Vuuren et al., 2007; Vestreng et al., 2007, 2009), but also on the nature of the aerosols.

Controversely, over SD and the ME the positive AOD trends are mainly caused by an increase of the natural dust. The WASO components reduce the total AOD trends in these regions due to the lower anthropogenic aerosol transport from Europe into this region. This results in a lower aerosol water content which also reduces the total AOD trends. The increase of the natural dust component to the total AOD does not only compensate for this reduction but also exceeds it, causing, as mentioned before, an overall positive trend over the desert-covered regions. The decrease of WASO components in these regions, potentially increases the aerosol lifetime due to the missing coating

ACPD
14, 26619–26653, 2014

effect (e.g. sulphate particles over dust) which makes the particles less susceptible for wet removal. This effect seems to play only a minor role here, as the AOD trends in the RCP00 and RCP85 simulations are similar, implying that the trends are strongly dominated by meteorological factors. Alternatively, the amount of hydrophilic coating material altering the dust could be sufficient in both scenarios from episodic pollution transport from Europe, such that the absolute amount of hydrophilic material, which might be different in both simulations, plays a minor role.

The simulation with the RCP85 scenario for SA and EC (see Fig. 6) reveals a reverse situation. The highly soluble WASO components and the water content exhibit a positive AOD trend while the dust component exhibits a negative trend with the overall AOD trend being positive in these two regions. The trends of the WASO components are very similar for the two regions while the aerosol water content trend over East China is nearly three times that of South Asia. This highlights either the strong hydrophilic nature of the aerosols over East China compared to that over South Asia or the occurrence of higher relative humidity causing more effective water uptake due to the exponential relationship between water uptake and relative humidity.

Finally, over SEA, the negative AOD trends are due to the decrease of all aerosol components (see Table 1). Dust and sea salt, however, show a significant decrease, implying trends driven by meteorological conditions. In particular, this trend is enhanced by the decrease of the aerosol water content (also significant), which is mostly due to the decrease of the highly soluble sea salt. Nevertheless, the BC/OC decrease (due to biomass burning decrease in the region during the 2001–2010 decade) enhances the negative trends by $\approx 0.4 \times 10^{-3}\,\mathrm{yr}^{-1}$ directly and indirectly decreasing even further the water uptake. Therefore the total trend in this region ($\approx 2.75 \times 10^{-3}\,\mathrm{yr}^{-1}$) is a combination of a meteorological effect and a decrease of the biomass burning emissions.

ACPD
14, 26619–26653, 2014

7 Conclusions

In this work, the AOD was simulated for a period of 10 years (2001–2010) with the EMAC Chemistry General Circulation Model. AODs from AERONET stations were used to evaluate the model results prior to the calculation of the global and regional AOD trends. Satellite retrievals from MODIS, Sea-WIFS and MISR have subsequently been used to estimate the AOD trends and compare them with the simulated results. Despite some clear differences between simulated and satellite-derived AOD trends, the general patterns of trends in the aerosol extinction are well reproduced, also on a regional level. Seven regions of interest are selected to conduct a regional analysis, based on the strength of the signal from both model and satellite AOD trends.

The main objective of this work is to identify the causes of the decadal AOD trends for the designated regions of interest by decomposing the AOD trends into its aerosol components trends. Therefore, two simulations have been performed to address the research objective; one with changing and one with constant emissions, using identical same atmospheric dynamics. The differences between the two simulations show that the observed AOD increases over Middle East and North Africa are caused mostly due to meteorological effects. A strong increase in the dust component of the AOD is found in both simulations for those regions. Over Eastern US and Western Europe, significant decreasing trends are deduced from the model simulation only when realistic, decreasing emissions in the decade 2001–2010 are included. This indicates the strong influence of anthropogenic emissions on aerosol load and the related AOD. Consequently, it can be confirmed that in Eastern US and Western Europe the AOD decrease is purely driven by emissions reduction policies.

For South Asia and East China the AOD trend is positive both from model results and satellite observations. The differences between the two model simulations identify that the AOD is increasing due to a combination of changes in the anthropogenic emissions and the meteorological conditions in the denoted areas. Finally, for South-East Asia, the decreasing trends are due to the decrease in the biomass burning emissions

ACPD
14, 26619–26653, 2014

and the meteorological conditions, where the purely meteorological trend contributes approximately 50 % of the total AOD trend. The role of natural aerosols (i.e. desert dust) has proven to be significant for Middle East and North Africa and non-negligible for China and South Asia. Future work in this area would include the online production of dust and sea salt emissions during the simulation time in order to identify the effects of meteorology in the dust component AOD by introducing emission variability for both sea salt and dust in the model. Even though the existing parameterizations for emissions of natural species hide a number of uncertainties, the comparison with the AOD trends that results from off-line prescribed inventories will identify the relative importance of the two methods (e.g. if the AOD trend from dust changes significantly).

Acknowledgements. The authors thank A. Kerkweg and P. Jöckel for their valuable work on the EMAC source code. The authors wish also to acknowledge the use of the Ferret program for analysis and graphics in this paper. Ferret is a product of NOAA's Pacific Marine Environmental Laboratory (information is available at http://www.ferret.noaa.gov). A. K. Georgoulias acknowledges financial support from the QUADIEEMS project which is co-financed by the European Social Fund (ESF) and national resources under the operational programme Education and Lifelong Learning (EdLL) within the framework of the Action "Supporting Postdoctoral Researchers".

The service charges for this open access publication have been covered by the Max Planck Society.

References

Abdou, W. A., Diner, D. J., Martonchik, J. V., Bruegge, C. J., Kahn, R. A., Gaitley, B. J., Crean, K. A., Remer, L. A., and Holben, B.: Comparison of coincident Multiangle Imaging Spectroradiometer and Moderate Resolution Imaging Spectroradiometer aerosol optical depths over land and ocean scenes containing Aerosol Robotic Network sites, J. Geophys. Res., 110, D10S07, doi:10.1029/2004JD004693, 2005. 26633

Andreae, M. O., Jones, C. D., and Cox, P. M.: Strong present-day aerosol cooling implies a hot future, Nature, 435, 1187–1190, 2005. 26620

ACPD

14, 26619–26653, 2014

Astitha, M., Lelieveld, J., Abdel Kader, M., Pozzer, A., and de Meij, A.: Parameterization of dust emissions in the global atmospheric chemistry-climate model EMAC: impact of nudging and soil properties, Atmos. Chem. Phys., 12, 11057–11083, doi:10.5194/acp-12-11057-2012, 2012. 26624, 26629, 26632

Cao, J., Garbaccio, R., and Ho, M. S.: China's 11th five-year plan and the environment: reducing SO_2 emissions, Review of Environmental Economics and Policy, 3, 231–250, 2009. 26621

Chin, M., Diehl, T., Tan, Q., Prospero, J. M., Kahn, R. A., Remer, L. A., Yu, H., Sayer, A. M., Bian, H., Geogdzhayev, I. V., Holben, B. N., Howell, S. G., Huebert, B. J., Hsu, N. C., Kim, D., Kucsera, T. L., Levy, R. C., Mishchenko, M. I., Pan, X., Quinn, P. K., Schuster, G. L., Streets, D. G., Strode, S. A., Torres, O., and Zhao, X.-P.: Multi-decadal aerosol variations from 1980 to 2009: a perspective from observations and a global model, Atmos. Chem. Phys., 14, 3657–3690, doi:10.5194/acp-14-3657-2014, 2014. 26623, 26629

Chu, D., Kaufman, Y., Ichoku, C., Remer, L., Tanré, D., and Holben, B.: Validation of MODIS aerosol optical depth retrieval over land, Geophys. Res. Lett., 29, doi:10.1029/2001GL013205, 2002. 26627

Chylek, P., Lohmann, U., Dubey, M., Mishchenko, M., Kahn, R., and Ohmura, A.: Limits on climate sensitivity derived from recent satellite and surface observations, J. Geophys. Res.-Atmos., 112, D24S04, doi:10.1029/2007JD008740, 2007. 26622

de Meij, A., Pozzer, A., and Lelieveld, J.: Trend analysis in aerosol optical depths and pollutant emission estimates between 2000 and 2009, Atmos. Environ., 51, 75–85, doi:10.1016/j.atmosenv.2012.01.059, 2012a. 26622, 26630

de Meij, A., Pozzer, A., Pringle, K., Tost, H., and Lelieveld, J.: EMAC model evaluation and analysis of atmospheric aerosol properties and distribution with a focus on the Mediterranean region, Atmos. Res., 114–115, 38–69, doi:10.1016/j.atmosres.2012.05.014, 2012b. 26625, 26628, 26629

Diner, D., Beckert, J., Reilly, T., Bruegge, C., Conel, J., Kahn, R., Martonchik, J., Ackerman, T., Davies, R., Gerstl, S., Gordon, H., Muller, J.-P., Myneni, R., Sellers, P., Pinty, B., and Verstraete, M.: Multi-angle Imaging SpectroRadiometer (MISR) instrument description and experiment overview, IEEE Geoscience and Remote Sensing Society, 36, 3113–3136, doi:10.1109/36.700992, 1998. 26627

Dubovik, O., Smirnov, A., Holben, B., King, M., Kaufman, Y., Eck, T., and Slutsker, I.: Accuracy assessments of aerosol optical properties retrieved from Aerosol Robotic Network

ACPD
14, 26619–26653, 2014

(AERONET) Sun and sky radiance measurements, J. Geophys. Res, 105, 9791–9806, 2000. 26628

Eck, T., Holben, B., Reid, J., Dubovik, O., Smirnov, A., O'Neill, N., Slutsker, I., and Kinne, S.: Wavelength dependence of the optical depth of biomass burning, urban, and desert dust aerosols, J. Geophys. Res, 104, 31333–31349, 1999. 26628

Gao, B.-C.: NDWI – a normalized difference water index for remote sensing of vegetation liquid water from space, Remote Sens. Environ., 58, 257–266, 1996. 26634

Granier, C., Bessagnet, B., Bond, T., D'Angiola, A., van der Gon, H. D., Frost, G. J., Heil, A., Kaiser, J. W., Kinne, S., Klimont, Z., Kloster, S., Lamarque, J.-F., Liousse, C., Masui, T., Meleux, F., Mieville, A., Ohara, T., Raut, J.-C., Riahi, K., Schultz, M.G., Smith, S. J., Thompson, A., van Aardenne, J., van der Werf, G.R., and van Vuuren D. P.: Evolution of anthropogenic and biomass burning emissions of air pollutants at global and regional scales during the 1980–2010 period, Climatic Change, 109, 163–190, 2011. 26626

Hinkelman, L. M., Stackhouse, P. W., Wielicki, B. A., Zhang, T., and Wilson, S. R.: Surface insolation trends from satellite and ground measurements: comparisons and challenges, J. Geophys. Res.-Atmos., 114, D00D20, doi:10.1029/2008JD011004, 2009. 26622

Holben, B. N., Eck, T. F., Slutsker, I., Tanré, D., Buis, J. P., Setzer, A., Vermote, E., Reagan, J. A., Kaufman, Y. J., Nakajima, T., Lavenu, F., Jankowiak, I., and Smirnov, A.: AERONET: federated instrument network and data archive for aerosol characterization, Remote Sens. Environ., 66, 1–16, 1998. 26628

Hsu, N. C., Tsay, S.-C., King, M. D., and Herman, J. R.: Aerosol properties over bright-reflecting source regions, IEEE T. Geosci. Remote, 42, 557–569, 2004. 26628

Hsu, N. C., Tsay, S.-C., King, M. D., and Herman, J. R.: Deep blue retrievals of Asian aerosol properties during ACE-Asia, IEEE T. Geosci. Remote, 44, 3180–3195, 2006. 26628

Hsu, N. C., Gautam, R., Sayer, A. M., Bettenhausen, C., Li, C., Jeong, M. J., Tsay, S.-C., and Holben, B. N.: Global and regional trends of aerosol optical depth over land and ocean using SeaWiFS measurements from 1997 to 2010, Atmos. Chem. Phys., 12, 8037–8053, doi:10.5194/acp-12-8037-2012, 2012. 26622, 26628, 26630

Jeuken, A., Siegmund, P., Heijboer, L., Feichter, J., and Bengtsson, L.: On the potential assimilating meteorological analyses in a global model for the purpose of model validation, J. Geophys. Res., 101, 16939–16950, 1996. 26626

Jöckel, P., Tost, H., Pozzer, A., Brühl, C., Buchholz, J., Ganzeveld, L., Hoor, P., Kerkweg, A., Lawrence, M. G., Sander, R., Steil, B., Stiller, G., Tanarhte, M., Taraborrelli, D.,

ACPD
14, 26619–26653, 2014

van Aardenne, J., and Lelieveld, J.: The atmospheric chemistry general circulation model ECHAM5/MESSy1: consistent simulation of ozone from the surface to the mesosphere, Atmos. Chem. Phys., 6, 5067–5104, doi:10.5194/acp-6-5067-2006, 2006. 26626

Jöckel, P., Kerkweg, A., Pozzer, A., Sander, R., Tost, H., Riede, H., Baumgaertner, A., Gromov, S., and Kern, B.: Development cycle 2 of the Modular Earth Submodel System (MESSy2), Geosci. Model Dev., 3, 717–752, doi:10.5194/gmd-3-717-2010, 2010. 26624, 26626, 26630

Kahn, R. A., Gaitley, B. J., Martonchik, J. V., Diner, D. J., Crean, K. A., and Holben, B.: Multiangle Imaging Spectroradiometer (MISR) global aerosol optical depth validation based on 2 years of coincident Aerosol Robotic Network (AERONET) observations, J. Geophys. Res., 110, 148–227, doi:10.1029/2004JD004706, 2005. 26627

Kahn, R. A., Garay, M. J., Nelson, D. L., Yau, K. K., Bull, M. A., Gaitley, B. J., Martonchik, J. V., and Levy, R. C.: Satellite-derived aerosol optical depth over dark water from MISR and MODIS: comparisons with AERONET and implications for climatological studies, J. Geophys. Res.-Atmos., 112, D18205, doi:10.1029/2006JD008175, 2007. 26633

Kahn, R. A., Nelson, D. L., Garay, M. J., Levy, R. C., Bull, M. A., Diner, D. J., Martonchik, J. V., Paradise, S. R., Hansen, E. G., and Remer, L. A.: MISR aerosol product attributes and statistical comparisons with MODIS, IEEE T. Geosci. Remote, 47, 4095–4114, 2009. 26633

Kahn, R. A., Gaitley, B. J., Garay, M., Diner, D. J., Eck, T. A. S., and Holben, B.: Multiangle Imaging Spectroradiometer (MISR) global aerosol optical depth validation based on 2 years of coincident Aerosol Robotic Network (AERONET) observations, J. Geophys. Res., 115, 148–227, doi:10.1029/2010JD014601, 2010. 26627

Kaufman, Y. J., Tanré, D., Remer, L. A., Vermote, E. F., Chu, A., and Holben, B. N.: Multiangle Imaging Spectroradiometer (MISR) global aerosol optical depth validation based on 2 years of coincident Aerosol Robotic Network (AERONET) observations, J. Geophys. Res., 102, 17051–17068, doi:10.1029/96JD03988, 1997. 26627

Kaufman, Y. J., Tanré, D., and Boucher, O.: A satellite view of aerosols in the climate system, Nature, 419, 215–223, 2002. 26620

Kerkweg, A., Buchholz, J., Ganzeveld, L., Pozzer, A., Tost, H., and Jöckel, P.: Technical Note: An implementation of the dry removal processes DRY DEPosition and SEDImentation in the Modular Earth Submodel System (MESSy), Atmos. Chem. Phys., 6, 4617–4632, doi:10.5194/acp-6-4617-2006, 2006a. 26625

ACPD
14, 26619–26653, 2014

Kerkweg, A., Sander, R., Tost, H., and Jöckel, P.: Technical note: Implementation of prescribed (OFFLEM), calculated (ONLEM), and pseudo-emissions (TNUDGE) of chemical species in the Modular Earth Submodel System (MESSy), Atmos. Chem. Phys., 6, 3603–3609, doi:10.5194/acp-6-3603-2006, 2006b. 26625

Kishcha, P., Starobinets, B., Kalashnikova, O., Long, C. N., and Alpert, P.: Variations of meridional aerosol distribution and solar dimming, J. Geophys. Res.-Atmos., 114, D00D14, doi:10.1029/2008JD010975, 2009. 26622

Lamarque, J., Kyle, G., Meinshausen, M., Riahi, K., Smith, S., van Vuuren, D., Conley, A., and Vitt, F.: Global and regional evolution of short-lived radiatively-active gases and aerosols in the representative concentration pathways, Climatic Change, 109, 191–212, doi:10.1007/s10584-011-0155-0, 2011. 26626

Lauer, A., Eyring, V., Hendricks, J., Jöckel, P., and Lohmann, U.: Global model simulations of the impact of ocean-going ships on aerosols, clouds, and the radiation budget, Atmos. Chem. Phys., 7, 5061–5079, doi:10.5194/acp-7-5061-2007, 2007. 26624

Lelieveld, J., Barlas, C., Giannadaki, D., and Pozzer, A.: Model calculated global, regional and megacity premature mortality due to air pollution, Atmos. Chem. Phys., 13, 7023–7037, doi:10.5194/acp-13-7023-2013, 2013. 26620

Levy, R. C., Remer, L. A., Kleidman, R. G., Mattoo, S., Ichoku, C., Kahn, R., and Eck, T. F.: Global evaluation of the Collection 5 MODIS dark-target aerosol products over land, Atmos. Chem. Phys., 10, 10399–10420, doi:10.5194/acp-10-10399-2010, 2010. 26627

Long, C. N., Dutton, E. G., Augustine, J., Wiscombe, W., Wild, M., McFarlane, S. A., and Flynn, C. J.: Significant decadal brightening of downwelling shortwave in the continental United States, J. Geophys. Res.-Atmos., 114, D00D06, doi:10.1029/2008JD011263, 2009. 26622

Lu, Z., Streets, D. G., Zhang, Q., Wang, S., Carmichael, G. R., Cheng, Y. F., Wei, C., Chin, M., Diehl, T., and Tan, Q.: Sulfur dioxide emissions in China and sulfur trends in East Asia since 2000, Atmos. Chem. Phys., 10, 6311–6331, doi:10.5194/acp-10-6311-2010, 2010. 26621, 26622

Meinshausen, M., Smith, S., Calvin, K., Daniel, J., Kainuma, M., Lamarque, J., Matsumoto, K., Montzka, S., Raper, S., Riahi, K., Thomson, A., Velders, G., and van Vuuren, D.: The RCP greenhouse gas concentrations and their extensions from 1765 to 2300, Climatic Change, 109, 213–241, doi:10.1007/s10584-011-0156-z, 2011. 26626

ACPD
14, 26619–26653, 2014

Mishchenko, M. I. and Geogdzhayev, I. V.: Satellite remote sensing reveals regional tropospheric aerosol trends, Opt. Express, 15, 7423–7438, 2007. 26622
Norris, J. R. and Wild, M.: Trends in aerosol radiative effects over China and Japan inferred from observed cloud cover, solar "dimming", and solar "brightening", J. Geophys. Res.-Atmos., 114, D00D15, doi:10.1029/2008JD011378, 2009. 26622
Ohmura, A.: Observed decadal variations in surface solar radiation and their causes, J. Geophys. Res.-Atmos., 114, D00D05, doi:10.1029/2008JD011290, 2009. 26622
Philandras, C. M., Nastos, P. T., Kapsomenakis, J., Douvis, K. C., Tselioudis, G., and Zerefos, C. S.: Long term precipitation trends and variability within the Mediterranean region, Nat. Hazards Earth Syst. Sci., 11, 3235–3250, doi:10.5194/nhess-11-3235-2011, 2011. 26632
Pinker, R., Zhang, B., and Dutton, E.: Do satellites detect trends in surface solar radiation?, Science, 308, 850–854, 2005. 26622
Pozzer, A., Jöckel, P., Sander, R., Williams, J., Ganzeveld, L., and Lelieveld, J.: Technical Note: The MESSy-submodel AIRSEA calculating the air–sea exchange of chemical species, Atmos. Chem. Phys., 6, 5435–5444, doi:10.5194/acp-6-5435-2006, 2006. 26625
Pozzer, A., Jöckel, P., Tost, H., Sander, R., Ganzeveld, L., Kerkweg, A., and Lelieveld, J.: Simulating organic species with the global atmospheric chemistry general circulation model ECHAM5/MESSy1: a comparison of model results with observations, Atmos. Chem. Phys., 7, 2527–2550, doi:10.5194/acp-7-2527-2007, 2007. 26624
Pozzer, A., de Meij, A., Pringle, K. J., Tost, H., Doering, U. M., van Aardenne, J., and Lelieveld, J.: Distributions and regional budgets of aerosols and their precursors simulated with the EMAC chemistry-climate model, Atmos. Chem. Phys., 12, 961–987, doi:10.5194/acp-12-961-2012, 2012. 26624, 26625, 26629
Pringle, K. J., Tost, H., Message, S., Steil, B., Giannadaki, D., Nenes, A., Fountoukis, C., Stier, P., Vignati, E., and Lelieveld, J.: Description and evaluation of GMXe: a new aerosol submodel for global simulations (v1), Geosci. Model Dev., 3, 391–412, doi:10.5194/gmd-3-391-2010, 2010a. 26624, 26625, 26629
Pringle, K. J., Tost, H., Pozzer, A., Pöschl, U., and Lelieveld, J.: Global distribution of the effective aerosol hygroscopicity parameter for CCN activation, Atmos. Chem. Phys., 10, 5241–5255, doi:10.5194/acp-10-5241-2010, 2010b. 26625
Ramanathan, V., Crutzen, P., Kiehl, J., and Rosenfeld, D.: Aerosols, climate, and the hydrological cycle, Science, 294, 5549, 2119–2124, doi:10.1126/science.1064034, 2001a. 26620

ACPD
14, 26619–26653, 2014

Ramanathan, V., Crutzen, P. J., Lelieveld, J., Mitra, A. P., Althausen, D., Anderson, J., Andreae, M. O., Cantrell, W., Cass, G. R., Chung, C. E., Clarke, A. D., Coakley, J. A., Collins, W. D., Conant, W. C., Dulac, F., Heintzenberg, J., Heymsfield, A. J., Holben, B., Howell, S., Hudson, J., Jayaraman, A., Kiehl, J. T., Krishnamurti, T. N., Lubin, D., McFarquhar, G., Novakov, T., Ogren, J. A., Podgorny, I. A., Prather, K., Priestley, K., Prospero, J. M., Quinn, P. K., Rajeev, K., Rasch, P., Rupert, S., Sadourny, R., Satheesh, S. K., Shaw, G. E., Sheridan, P., and Valero, F. P. J., Remer, L. A., Tanré, D., Kaufman, Y. J., Ichoku, C., Mattoo, S., Levy, R., Chu, D. A., Holben, B., Dubovik, O., Smirnov, A., Martins, J. V., Li, R.-R., and Ahmad, Z.: Indian Ocean Experiment: an integrated analysis of the climate forcing and effects of the great Indo-Asian haze, J. Geophys. Res.-Atmos., 106, 28371–28398, 2001b. 26620

Remer, L., Kleidman, R., Levy, R., Kaufman, Y., Tanré, D., Mattoo, S., Martins, J., Ichoku, C., Koren, I., Yu, H., and Holben, B.: Global aerosol climatology from the MODIS satellite sensors, J. Geophys. Res., 113, D14S07, doi:10.1029/2007JD009661, 2008. 26622, 26627

Remer, L. A., Tanré, D., Kaufman, Y. J., Ichoku, C., Mattoo, S., Levy, R., Chu, D. A., Holben, B., Dubovik, O., Smirnov, A., Martins, J. V., Li, R.-R., and Ahmad, Z.: Validation of MODIS aerosol retrieval over ocean, Geophys. Res. Lett., 29, doi:10.1029/2001GL013204, 2002. 26627

Remer, L. A., Kaufman, Y. J., Tanré, D., Mattoo, S., Chu, D. A., Martins, J. V., Li, R.-R., Ichoku, C., Levy, R. C., Kleidman, R. G., Eck, T. F., Vermote, E., and Holben, B. N.: The MODIS aerosol algorithm, products, and validation., J. Atmos. Sci., 62, 947–973, doi:10.1175/JAS3385.1, 2005. 26627

Roeckner, E., Brokopf, R., Esch, M., Giorgetta, M., Hagemann, S., Kornblueh, L., Manzini, E., Schlese, U., and Schulzweida, U.: Sensitivity of simulated climate to horizontal and vertical resolution in the ECHAM5 atmosphere model, J. Climate, 19, 3771–3791, 2006. 26624

Sander, R., Kerkweg, A., Jöckel, P., and Lelieveld, J.: Technical note: The new comprehensive atmospheric chemistry module MECCA, Atmos. Chem. Phys., 5, 445–450, doi:10.5194/acp-5-445-2005, 2005. 26625

Sander, R., Baumgaertner, A., Gromov, S., Harder, H., Jöckel, P., Kerkweg, A., Kubistin, D., Regelin, E., Riede, H., Sandu, A., Taraborrelli, D., Tost, H., and Xie, Z.-Q.: The atmospheric chemistry box model CAABA/MECCA-3.0, Geosci. Model Dev., 4, 373–380, doi:10.5194/gmd-4-373-2011, 2011. 26625

Sayer, A., Hsu, N., Bettenhausen, C., Ahmad, Z., Holben, B., Smirnov, A., Thomas, G., and Zhang, J.: SeaWiFS Ocean Aerosol Retrieval (SOAR): algorithm, validation, and comparison

ACPD
14, 26619–26653, 2014

with other data sets, J. Geophys. Res.-Atmos., 117, D03206, doi:10.1029/2011JD016599, 2012a. 26628
Sayer, A. M., Hsu, N. C., Bettenhausen, C., Jeong, M.-J., Holben, B. N., and Zhang, J.: Global and regional evaluation of over-land spectral aerosol optical depth retrievals from SeaWiFS, Atmos. Meas. Tech., 5, 1761–1778, doi:10.5194/amt-5-1761-2012, 2012b. 26628
Shehadeh, N. and Ananbeh, S.: The impact of climate change upon winter rainfall, Am. J. Environ. Sci., 9, 73–81, 2013. 26632
Tanré, D., Kaufman, Y. J., Herman, M., and Mattoo, S.: Multiangle Imaging Spectroradiometer (MISR) global aerosol optical depth validation based on 2 years of coincident Aerosol Robotic Network (AERONET) observations, J. Geophys. Res., 102, 16971–16988, doi:10.1029/96JD03437, 1997. 26627
Tiao, G., Reinsel, G., Xu, D., Pedrick, J., Zhu, X., Miller, A., DeLuisi, J., Mateer, C., and Wuebbles, D.: Effects of autocorrelation and temporal sampling schemes on estimates of trend and spatial correlation, J. Geophys. Res.-Atmos., 95, 20507–20517, 1990. 26630
Tost, H., Jöckel, P., Kerkweg, A., Pozzer, A., Sander, R., and Lelieveld, J.: Global cloud and precipitation chemistry and wet deposition: tropospheric model simulations with ECHAM5/MESSy1, Atmos. Chem. Phys., 7, 2733–2757, doi:10.5194/acp-7-2733-2007, 2007. 26625
van der Werf, G. R., Randerson, J. T., Giglio, L., Collatz, G. J., Mu, M., Kasibhatla, P. S., Morton, D. C., DeFries, R. S., Jin, Y., and van Leeuwen, T. T.: Global fire emissions and the contribution of deforestation, savanna, forest, agricultural, and peat fires (1997–2009), Atmos. Chem. Phys., 10, 11707–11735, doi:10.5194/acp-10-11707-2010, 2010. 26625
van Vuuren, D. P., Den Elzen, M. G., Lucas, P. L., Eickhout, B., Strengers, B. J., van Ruijven, B., Wonink, S., and van Houdt, R.: Stabilizing greenhouse gas concentrations at low levels: an assessment of reduction strategies and costs, Climatic Change, 81, 119–159, 2007. 26634
van Vuuren, D., Edmonds, J., Kainuma, M., Riahi, K., Thomson, A., Hibbard, K., Hurtt, G., Kram, T., Krey, V., Lamarque, J.-F., Masui, T., Meinshausen, M., Nakicenovic, N., Smith, S., and Rose, S.: The representative concentration pathways: an overview, Climatic Change, 109, 5–31, doi:10.1007/s10584-011-0148-z, 2011a. 26626
van Vuuren, D., Edmonds, J., Kainuma, M., Riahi, K., and Weyant, J.: A special issue on the RCPs, Climatic Change, 109, 1–4, doi:10.1007/s10584-011-0157-y, 2011b. 26626

ACPD
14, 26619–26653, 2014

Vestreng, V., Myhre, G., Fagerli, H., Reis, S., and Tarrasón, L.: Twenty-five years of continuous sulphur dioxide emission reduction in Europe, Atmos. Chem. Phys., 7, 3663–3681, doi:10.5194/acp-7-3663-2007, 2007. 26632, 26634

Vestreng, V., Ntziachristos, L., Semb, A., Reis, S., Isaksen, I. S. A., and Tarrasón, L.: Evolution of NO_x emissions in Europe with focus on road transport control measures, Atmos. Chem. Phys., 9, 1503–1520, doi:10.5194/acp-9-1503-2009, 2009. 26632, 26634

Weatherhead, E. C., Reinsel, G. C., Tiao, G. C., Meng, X.-L., Choi, D., Cheang, W.-K., Keller, T., DeLuisi, J., Wuebbles, D. J., Kerr, J. B., Miller, A. J., Oltmans, S. J., and Frederick, J. E.: Factors affecting the detection of trends: statistical considerations and applications to environmental data, J. Geophys. Res.-Atmos., 103, 17149–17161, 1998. 26629, 26630

Weatherhead, E. C., Stevermer, A. J., and Schwartz, B. E.: Detecting environmental changes and trends, Phys. Chem. Earth, 27, 399–403, 2002. 26630

Wild, M.: Introduction to special section on global dimming and brightening, J. Geophys. Res.-Atmos., 115, D00D00, doi:10.1029/2009JD012841, 2010. 26620, 26622

Wild, M., Gilgen, H., Roesch, A., Ohmura, A., Long, C. N., Dutton, E. G., Forgan, B., Kallis, A., Russak, V., and Tsvetkov, A.: From dimming to brightening: decadal changes in solar radiation at Earth's surface, Science, 308, 847–850, 2005. 26620, 26622

Yoon, J. and Pozzer, A.: Model-simulated trend of surface carbon monoxide for the 2001–2010 decade, Atmos. Chem. Phys., 14, 10465–10482, doi:10.5194/acp-14-10465-2014, 2014. 26634

Yoon, J., von Hoyningen-Huene, W., Kokhanovsky, A. A., Vountas, M., and Burrows, J. P.: Trend analysis of aerosol optical thickness and Ångström exponent derived from the global AERONET spectral observations, Atmos. Meas. Tech., 5, 1271–1299, doi:10.5194/amt-5-1271-2012, 2012. 26628

Yoon, J., Burrows, J. P., Vountas, M., von Hoyningen-Huene, W., Chang, D. Y., Richter, A., and Hilboll, A.: Changes in atmospheric aerosol loading retrieved from space-based measurements during the past decade, Atmos. Chem. Phys., 14, 6881–6902, doi:10.5194/acp-14-6881-2014, 2014. 26630, 26631, 26633

Zhang, J. and Reid, J. S.: A decadal regional and global trend analysis of the aerosol optical depth using a data-assimilation grade over-water MODIS and Level 2 MISR aerosol products, Atmos. Chem. Phys., 10, 10949–10963, doi:10.5194/acp-10-10949-2010, 2010. 26622, 26630

ACPD
14, 26619–26653, 2014

Zhang, Q., Streets, D. G., Carmichael, G. R., He, K. B., Huo, H., Kannari, A., Klimont, Z., Park, I. S., Reddy, S., Fu, J. S., Chen, D., Duan, L., Lei, Y., Wang, L. T., and Yao, Z. L.: Asian emissions in 2006 for the NASA INTEX-B mission, Atmos. Chem. Phys., 9, 5131–5153, doi:10.5194/acp-9-5131-2009, 2009. 26622

ACPD
14, 26619–26653, 2014

Table 1. Regional trend estimates of RCP85-based AODs, i.e. total, black carbon (BC), organic carbon (OC), dust (DU), water soluble (WASO), H_2O, and sea salt AODs, in 10^{-3} year^{-1}. The 1 SD is also shown. Bold type indicates the significant trend within 95 % of confidence levels.

Region	total	BC	OC	DU	WASO	H_2O	SS
(a) EUS	**−5.542 ± 0.489**	**−0.034 ± 0.002**	−0.033 ± 0.033	−0.004 ± 0.019	**−1.337 ± 0.112**	**−4.111 ± 0.434**	−0.022 ± 0.016
(b) WE	**−4.674 ± 0.619**	**−0.042 ± 0.003**	**−0.098 ± 0.016**	−0.065 ± 0.282	**−0.923 ± 0.144**	**−3.498 ± 0.408**	**−0.046 ± 0.011**
(c) SD	**+1.299 ± 0.611**	−0.000 ± 0.002	−0.018 ± 0.016	**+1.927 ± 0.609**	**−0.272 ± 0.88**	−0.325 ± 0.199	−0.009 ± 0.006
(d) ME	+0.587 ± 0.484	**+0.009 ± 0.001**	**−0.025 ± 0.007**	**+0.754 ± 0.316**	−0.079 ± 0.070	−0.070 ± 0.260	**−0.001 ± 0.001**
(e) SA	+1.524 ± 0.876	+0.011 ± 0.006	+0.001 ± 0.040	−0.489 ± 0.263	**+0.818 ± 0.209**	**+1.236 ± 0.564**	**−0.054 ± 0.023**
(f) EC	**+5.403 ± 1.749**	**+0.099 ± 0.017**	+0.012 ± 0.121	**−0.410 ± 0.188**	**+0.897 ± 0.317**	**+4.850 ± 1.488**	**−0.046 ± 0.015**
(g) SEA	−2.753 ± 1.474	−0.050 ± 0.037	−0.363 ± 0.301	**−0.027 ± 0.012**	−0.300 ± 0.197	**−1.907 ± 0.911**	**−0.104 ± 0.035**
(h) NH	**−0.798 ± 0.247**	**−0.005 ± 0.002**	**−0.062 ± 0.030**	−0.018 ± 0.037	**−0.126 ± 0.038**	**−0.565 ± 0.166**	**−0.020 ± 0.004**
(i) SH	−0.164 ± 0.139	+0.001 ± 0.003	+0.009 ± 0.033	**−0.017 ± 0.005**	+0.013 ± 0.029	−0.143 ± 0.075	**−0.027 ± 0.004**
(j) GL	**−0.481 ± 0.140**	−0.002 ± 0.002	−0.026 ± 0.023	−0.018 ± 0.017	**−0.056 ± 0.022**	**−0.354 ± 0.094**	**−0.024 ± 0.002**

ACPD
14, 26619–26653, 2014

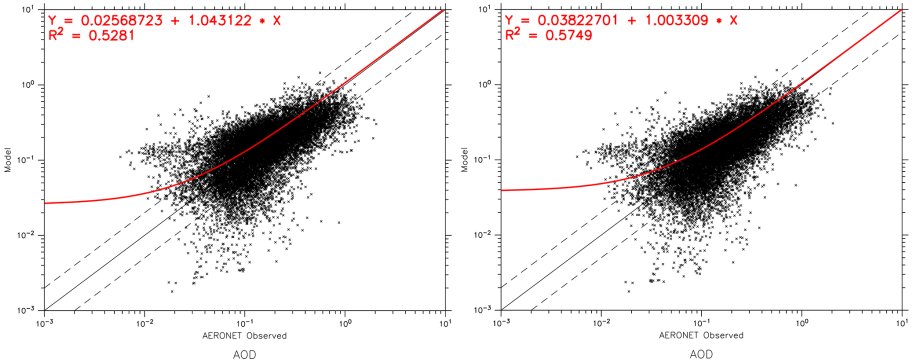

Figure 1. Scatter plot of observed (AERONET) and simulated daily AOD. The model is sampled in the same temporal/spatial location of the observations. The red line represent the linear fit, with the coefficient listed in the figure. Left: model results from simulation RCP00. Right: model results from simulation RCP85.

ACPD
14, 26619–26653, 2014

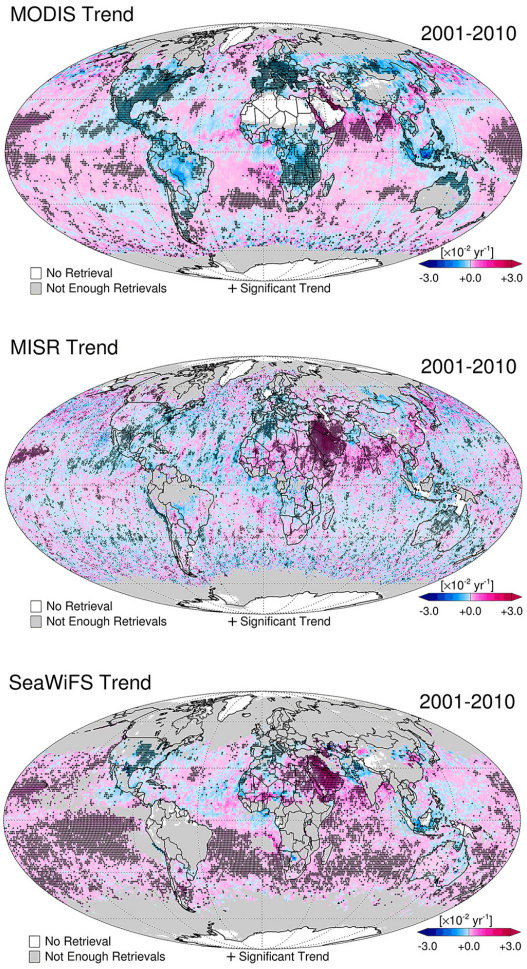

Figure 2. Linear trend between 2001–2010 in 10^{-2} year^{-1} from different satellite instrument.

ACPD
14, 26619–26653, 2014

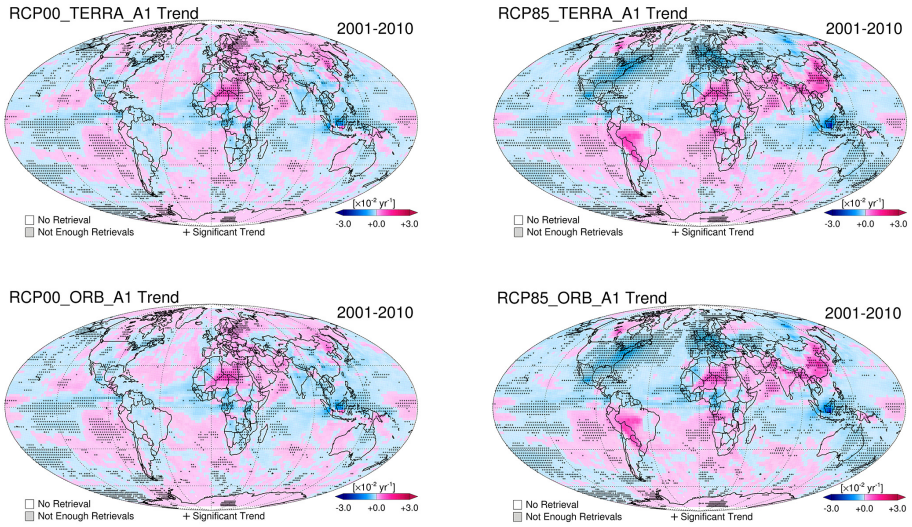

Figure 3. Linear trend between 2001–2010 in 10^{-2} year^{-1} for simulations RCP00 and RP85 (left and right column respectively) estimated using the output of the sumodel SORBIT, i.e. at the correct overpass time of the TERRA and OrbView-2 platform.

ACPD
14, 26619–26653, 2014

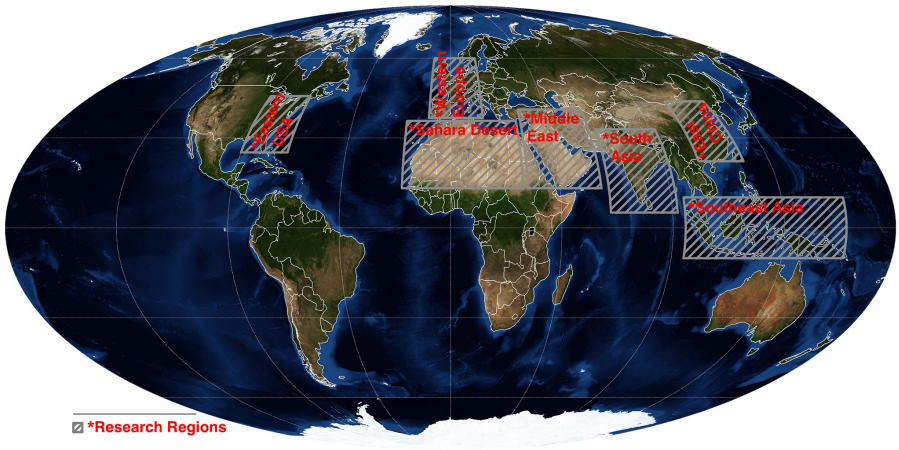

Figure 4. Regions used in this work.

ACPD
14, 26619–26653, 2014

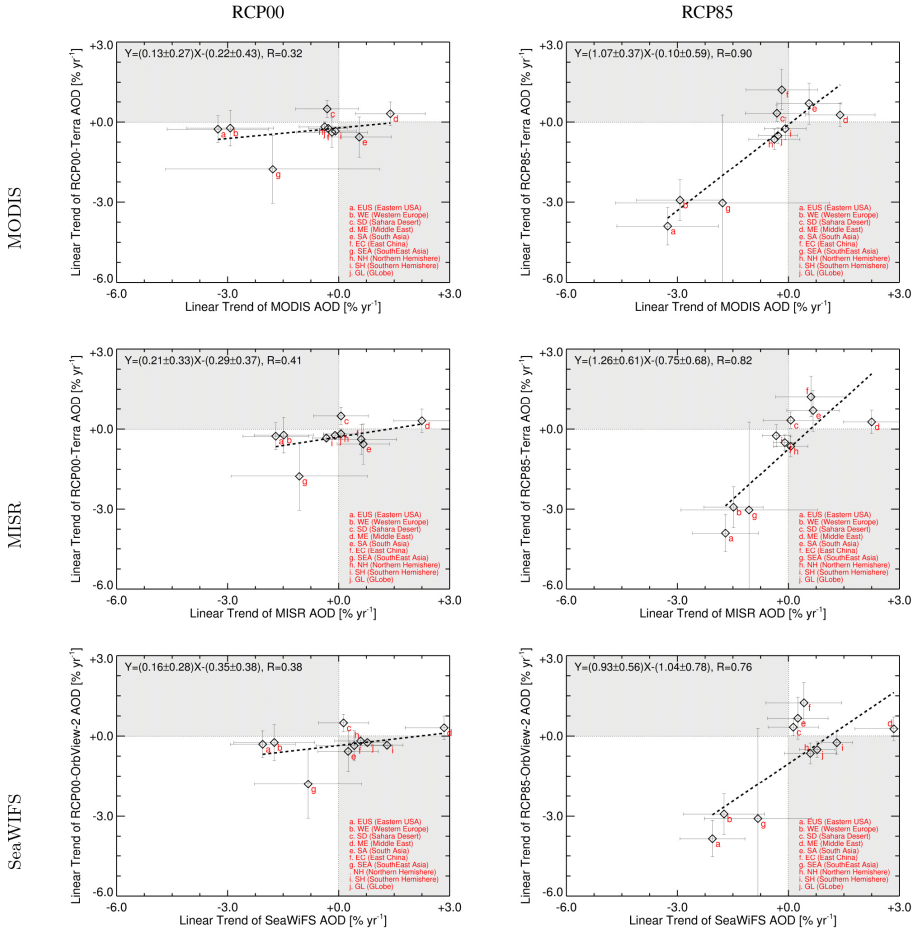

Figure 5. Linear trend between 2001–2010 in 10^{-2} year^{-1} by regions from model and satellite observations. The bars represent the 2σ (i.e. 2 SD) of the trends.

ACPD
14, 26619–26653, 2014

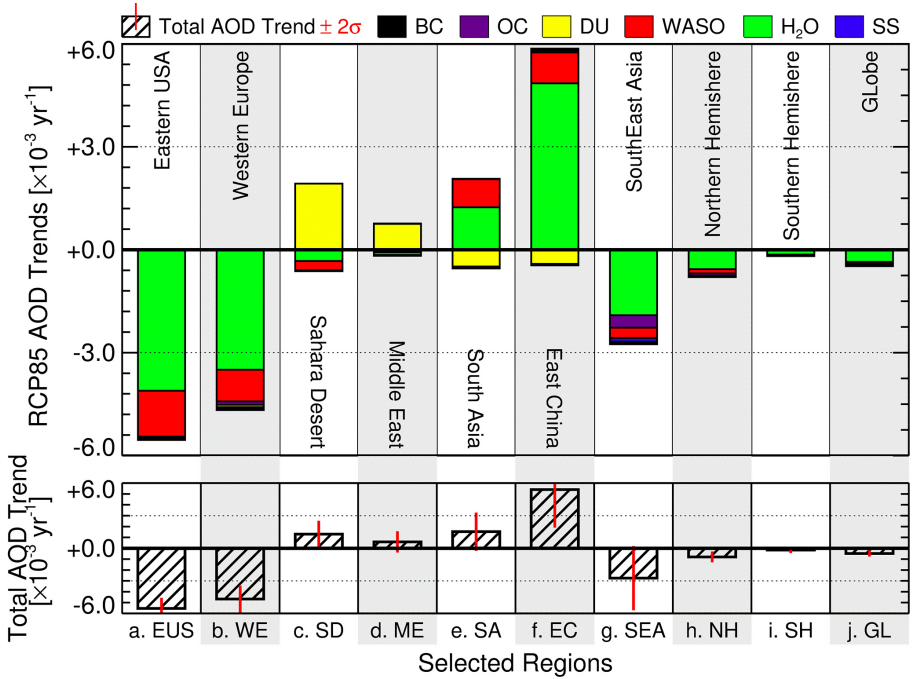

Figure 6. AOD changes between 2001–2010 for different regions and species.

ACPD
14, 26619–26653, 2014